AIIM

Association for Information and Image Management

1100 Wayne Avenue, Suite 1100
Silver Spring, Maryland 20910
301/587-8202

Centimeter

1 2 3 4 5 6 7 8 9 10 11 12 13 14 15 mm

1 2 3 4 5

Inches

1.0 1.1 1.25 1.4 1.6 1.8 2.0 2.2 2.5 2.8 3.2 3.6 4.0 4.5 5.0 5.6 6.3 7.1 8.0

MANUFACTURED TO AIIM STANDARDS
BY APPLIED IMAGE, INC.

1 of 1

DOE/BC/14951--7

Integrated Approach Towards the Application of Horizontal Wells to Improve Waterflooding Performance

Submitted by

The University of Tulsa
Tulsa, Oklahoma 74104

14951-7

Principal Investigator : Balmohan G. Kelkar
Co-Principal Investigators: Chris Liner, Dennis Kerr

Contract Date : January 1, 1993
Completion Date : December 31, 1996
Reporting Period : April 1 - June 30, 1994

Contracting Officer's Representative

Ms. Rhonda P. Lindsey
U.S. Department of Energy
Bartlesville Project Office
P. O. Box 1398
Bartlesville, OK 74005

Objectives

The overall purpose of the proposed project is to improve secondary recovery performance of a marginal oil field through the use of a horizontal injection well. The location and direction of the well will be selected based on the detailed reservoir description using integrated approach. We expect that 2 to 5% of original oil in place will be recovered using this method. This should extend the life of the reservoir by at least 10 years.

To accomplish the goals of the project, it is divided into two stages. In Stage I, we will select part of the Glenn Pool field (William B. Self Unit), and collect additional reservoir data by conducting cross bore hole tomography surveys and formation micro scanner logs through newly drilled well. In addition, we will also utilize analogous outcrop data. By combining the state of the art data with conventional core and log data, we will develop a detailed reservoir description based on integrated approach. After conducting extensive reservoir simulation studies, we will select a location and direction of a horizontal injection well. The well will be drilled based on optimized design, and the field performance will be monitored for at least six months. If the performance is encouraging, we will enter into second budget period of the project.

If continued, the second budget period of the project will involve selection of part of the same reservoir (Berryhill Unit - Tract 7), development of reservoir description using only conventional data, simulation of flow performance using developed reservoir description, selection of a location and direction of a horizontal injection well, and implementation of the well followed by monitoring of reservoir performance.

By comparing the results of two budget periods, we will be able to evaluate the utility of collecting additional data using state-of the-art technology. In addition, we will also be able to evaluate the application of horizontal wells in improving secondary recovery performance of marginal oil fields.

A successful completion of this project will provide new means of extending the life of marginal oil fields using easily available technology. It will also present a methodology to integrate various qualities and quantities of measured data to develop a detailed reservoir description.

Summary of Technical Progress

The overall report is divided into three sections. In the first section, we discuss the geological description and interpretation of well #82. In the next section, the progress on geophysical interpretation of cross bore hole seismic surveys is reported. In the last section, construction of reservoir description using geostatistical procedures and the flow simulation results are presented.

Geological Description and Interpretation
(By Dennis Kerr and Liangmiao Ye)

Executive Summary

Geological description and interpretation has focused on data compilation, analysis, and interpretation from the Self No. 82 well drilled in first quarter, 1994. Early analysis results indicated that discrete genetic intervals (DGI) C, D, and E offer the best potential for additional oil reserves. At the Self No. 82 well location, DGI C is represented by channel-fill facies which revealed actively bleeding oil from sandstone beds between lateral-accretion-surface-draping mudstone interbeds, and which revealed flushed oil from cross-stratified sandstones of the lower channel-fill subfacies. In DGI D, 22 ft. of sandstones are from the splay facies; however, only a 4 ft. thick sandstone appears to have been contacted by waterflooding at the Self No. 82 location (results from the high-resolution FMI log analysis, and not obvious from conventional log suite). FMI analysis has constrained the spatial orientation of architectural elements in the vicinity of Self No. 82 well. Using the results from core studies and FMI analysis a detailed facies architecture is being constructed for the interwell region in the vicinity of Self No. 82 well.

Core Studies

Whole core collected in the Self No. 82 well has been fully documented. Documentation includes detailed sedimentologic description and color photography. Core-plug remnants have been submitted for thin-section cutting. Selected intervals were loaned to DOE-NIPER for CATSCAN analysis.

Core observations of sandstones from discrete genetic intervals (DGI) A and B have bearing on the production potential of the upper most part of the Glenn Sand. Oil in the sandstone pores appears to be degraded and immobile. Thus, the upper 14 feet of the Glenn Sand is not likely being swept by the present water-flood program, at least in the vicinity of the Self No. 82 well.

Facies/subfacies descriptions for the reservoir sandstones have been refined as a result of the analysis of the Self No. 82 core. See Figure 1.

•Channel-fill facies (encountered in DGI A, B, and C):

Upward-fining texture. Upward decrease in scale of physical sedimentary structures. Upward increase in proportion of mudstone interbeds. Carbonaceous debris common throughout.

Lower channel-fill subfacies: well to moderately sorted medium-grained sandstone with medium-scale (2 to 8 in.; 5 to 20 cm.) cross stratification. Mudstone drapes common on cross strata.

Middle channel-fill subfacies: moderately sorted, lower medium-grained to poorly sorted, silty fine-grained sandstones with horizontal to low-angle parallel stratification and ripple lamination. Medium- to very-thin-bedded (1 to 6 in.; 2 to 15 cm.) mudstones to silty mudstones drape lateral accretion surfaces.

Upper channel-fill subfacies: mudstone to silty claystone.

•Splay facies (encountered in DGI D and E):

Upward-coarsening texture from fine-grained to medium-grained sandstone. Upward increase in stratal thickness in lower levels only; otherwise, irregular vertical stacking of thick to thin beds (0.4 to 2.5 ft.; 8 to 75 cm.). Ripple lamination and low-angle parallel bedding dominated; medium-scale cross stratification and contorted bedding less common. Thin bedded (0.1 to 0.4 ft.; 3 to 8 cm.) mudstones interstratified with sandstones throughout. DGI D includes more numerous mudstone drapes and thin laminations as compared to DGI E.

Oil staining observed in the Self No. 82 core largely correlates with facies/subfacies characteristics. In DGI C, actively bleeding oil corresponds to the sandstones between mudstone drapes on lateral accretion surfaces within the middle channel-fill subfacies. By contrast, the cross-stratified sandstones of the lower channel-fill subfacies appear to be flushed. In DGI D, actively bleeding oil was observed from all but one 4 ft. thick sandstone; each interval is divided by interstratified mudstones (see FMI analysis - Figure 2). Thus, facies/subfacies characteristics appear to be influential in oil saturation of the Glenn Sand.

FMI Analysis

Analysis of the microresistivity imaging log (FMI) collected in the Self No. 82 well is nearly complete. Efforts to date have focused on DGI C, D, and E because these units appear to have the highest potential for addition oil recovery.

The following list summarizes our conclusions thus far:

Structural dip azimuth averages 153° and dip angle 4°.

DGI C:

Lower channel-fill subfacies cross strata average dip azimuth 121°.

Lateral accretion surface average dip azimuth 150°.

Lateral accretion surface dip azimuth shows progressive upward rotation from 200° to 146°.

Angle of dip azimuth between cross strata and lateral accretion surface indicates a downstream location with increasing amplitude in thalweg sinuosity.

From spatial orientation and vertical spacing, it is expected that 19 lateral accretion mudstone drapes are present between Self No. 82 and Self No. 81 wells.

DGI D:

Divided into 4 splay units based on orientation patterns and separation by thin mudstone beds.

Relative Level	Dispersal Orientation
highest	southeast
	northwest
	northeast
lowest	southwest

Of the 22 ft of thickness, only a 4 ft. interval appears to be washed by water flooding. Not obvious in conventional log suite, but confirmed in core studies.

DGI E:

Divided into 2 splay units based on orientation patterns.

Relative Level	Dispersal Orientation
higher	south
lower	northeast

The lower splay of the two appears to have markedly higher water saturation.

Near-Term Goals

Detailed facies architecture is being constructed for the immediate vicinity of Self No. 82 well. In light of the findings from the advanced technology collected from the project participation in drilling the Self No. 82, facies architecture will provide an accurate configuration of the level of heterogeneity for each facies/subfacies. This detail will assist in developing a reservoir management plan for the Self Unit, and will be completed in early third-quarter of 1994.

Geophysical Interpretation of Field Survey
(By Chris L. Liner, Gokay Bozkurt and A. Shatilo)

Summary

Initial tomography results are available from Amoco, University of Tulsa, Memorial University and the University of Utah. All results agree that a strong P-wave anisotropy effect is present in several intervals above the Glenn Sand.

First arrival travel time data were processed to yield three tomograms between the crosswell survey wells (63-82, 82-64, 81-82). An initial comparison with the Amoco tomogram (63-82) displayed velocity agreement within 10%. However, artifacts due to unaccounted anisotropy in the tomography algorithm degraded the image quality in the University of Tulsa (TU) tomograms. The initial tomogram results from Memorial University show promising lateral variations within the Glenn. These appear to indicate geological changes. Interpretation is proceeding with the geological team (Kerr and Ye).

From core plug analysis, there is a strong correlation between velocity (P-wave), porosity, and permeability. Combined with tomography results, these petrophysical relationships will allow computation of interwell images of porosity and permeability in the Glenn Sand.

Overview and Anisotropy Discussion (C. Liner)

The geophysical efforts at Glenn Pool have progressed during the second quarter of 1994. This was a period of data processing and initial interpretation.

In the area of data processing, we currently have tomography results from Amoco (A. Vassiliou) and Memorial University of Newfoundland (L. Lines), and the University of Utah (G. Schuster). The Amoco results were introduced in the previous report (first quarter 94). The Memorial University tomograms are not yet complete. This work was discussed at length at a meeting in Tulsa between Dr. Lines and TU team members on June 29, 1994. Our initial assessment is that this result is significantly different from the Amoco result, particularly the level of detail in lateral variations of velocity. The origin of this tomogram is being forwarded to TU for final display and interpretation. Memorial University results for the other surveys will be available soon.

At The University of Tulsa, we are currently processing the data with a public-domain processing package (BOMTOM). This is discussed by G. Bozkurt below. The general approach involved first arrival data picking by Amoco. These time picks were E-mailed to TU and forwarded, along with deviation surveys and the 82 sonic log, to researchers in Newfoundland and Utah.

It was quickly apparent that the data presented a difficult geophysical problem because of strong P-wave anisotropy present in shaly rocks above the Glenn Sand. This was first recognized by A. Vassiliou of Amoco, and independently discovered by L. Lines of Memorial University. The following discussion is based on ideas originated by A. Vassiliou.

P-wave anisotropy means that the velocity of P-waves depend on direction of propagation. It is customary to refer to speed of horizontally traveling P-waves as Vh (horizontal velocity) and vertically traveling ones as Vv. If $Vh \approx Vv$ then the rocks are said to be weakly anisotropic, while $Vh >> Vv$ indicates strong anisotropy. In the Glenn Sand itself, we observe negligible anisotropy. However, the presence of strong anisotropy above the Glenn must be accounted for if accurate tomography results are to be obtained. Furthermore, the level of anisotropy observed at Glennpool is such that surface reflection data (such as 3-D seismic) may require special processing. For independent operators in the area, this fact could be very important at the interest in shallow 3-D seismic intensifies.

Velocity anisotropy is usually indirectly indicated. This can be through core plug measurements at frequencies 100 times (or more) greater than surface seismic frequencies, or tomographic results which are highly processed products, or even non-hyperbolic normal moveout curves on surface seismic data. At Glennpool we have rare direct evidence of strong P-wave anisotropy.

The first piece of evidence is the sonic log on the interval 1200 - 1600. Sonic logs measure velocity by refracting a high-frequency P-wave pulse vertically along wall of the borehole. Thus, sonic measurements indicate Vv. For example at the 1250 ft level in well 82 the sonic reading is 90 microsecs/ft, corresponding to a Vv of 11,110 ft/sec.

From the crosswell data, we can extract traces which have source and receiver at the same level (depth). The pertinent wells at Glennpool were surface surveyed to determine relative well-head location, and a deviation survey was run on each to track subsurface (x,y,z) coordinates of each well-bore. From this information, it is possible to construct a constant-level gather for each survey. Since the source and receiver for each trace are at the same depth, the direction of energy travel is horizontal and therefore indicates Vh. One way of displaying this information is shown in Figures 3. In this Figure the combination of horizontal distance and travel time has been combined to provide a Vh Pseudo-Sonic reading in microsecs/ft. For example, at the 1250 ft level in the 82->64 survey, the first arrival energy indicates a Vh Ps-Sonic value of about 71.5

microsecs/ft, corresponding to a *Vv* of 13,990 ft/sec. Note the consistency of this *Vh* Ps-Sonic value at the 1250 ft level in all three surveys.

To summarize, the sonic log in well 82 gives *Vv*=11,110 ft/s at 1250 ft while the crosswell data shows that *Vh*=13,990 ft/s at the same depth. This represents direct evidence for a *Vh* about 26% greater (26% anisotropy) than *Vv* in the rocks at this level. Generally, P-wave anisotropy greater than 10% is rare, which makes the level of anisotropy seen at Glennpool quite remarkable.

In the next section, progress in computing tomograms at TU and comparing tomograms from other workers is discussed. In the last section, core plug data are shown to exhibit a strong correlation between porosity, and permeability. These basic results lay the foundation for creating interwell porosity and permeability maps from the velocity tomograms.

TU Processing and Tomogram Comparison

Commonly, a geophysical procedure involves three steps: data acquisition, data processing, and data interpretation. Crosswell data from the Glenn Pool field were acquired during 4 days of field work in late January, 1994. The geophysical work between March-June 1994 involved mainly data processing.

First arrival travel times from "common source gathers" were picked by Amoco. Figure 4 shows a direct arrival picking process where the points are marked with a line. Each pick was recorded with its source-receiver depth. A data set of source-receiver coordinates and travel times were transferred to parties involved in processing. Table 1 shows the number of travel time picks and acquisition aperture for the three crosswell surveys.

Table 1

Traveltime Data Information For Three Survey Well Pairs

Well Pair	Source Coverage (ft)	Receiver Coverage (ft)	Number of Traveltimes
63-82	1220-1580	1108-1920	17759
82-64	1120-1920	1216-1568	14736
81-82	1220-1576	1084-1920	18898

The tomographic imaging software for data processing was provided by the U.S. Department of the Interior, Bureau of Mines as part of their technology transfer. The program is installed in the TU Geosciences Department Apollo workstation network for current research purposes.

BOMTOM (**B**ureau **O**f Mines **TOM**ography) is a straight ray tomographic image reconstruction program using a SIRT (Simultaneous Iterative Reconstruction Technique) algorithm. A generalized flowchart of the program is given in Figure 4.

All three TU tomograms between the survey wells (63-82, 82-64, and 81-82) were created using a 30-iteration BOMTOM run. A constant velocity of 10000 ft/s is used as an initial starting model. Maximum and minimum calculated velocities allowed are 10000 ft/s and 16000 ft/s, respectively. No other constraints are applied. Rest of the program parameters are left as default.

Figure 5 is the velocity tomogram between wells 63 and 82 created by TU. Same data were processed by Amoco and Memorial University of Newfoundland (MUN). There are significant differences between the tomograms because they are processed with different methods (all used Amoco time picks). However, Figure 6 shows a velocity profile comparison between Amoco and TU tomograms at a point 181 ft from well 63. Velocities are within a 10% agreement. Due to sampling differences the MUN result has not been incorporated into this figure.

Figure 7 is the velocity tomogram between wells 82 and 64. Survey wells 64, 82 and 63 are aligned in an approximate North-South direction. Crosswell acquisition geometry provided a continuous North-South image by simply combining the two tomograms side by side. Similar tomogram is also obtained between wells 81 and 82.

Future Work

The deviation survey will be incorporated into the input file for more accurate source-receiver coordinates. Well log information will be used to define a better starting model. Different processing results from TU, Amoco and MUN will be displayed in the same graphical format for better comparison. Finally, the tomograms will be interpreted in collaboration with the geological team.

Rock Property Measurements

Core plugs from Glenn Pool test well #82 were taken from depths between 1422 ft. and 1573 ft. Core interval from 1424 ft. to 1470 ft. is represented mainly by shale. Interval of the core between 1482 ft. and 1573 ft. corresponds to Glenn Pool sandstone. Total number of plugs is equal to 181. 45 of them represents shale and 136 sandstone. Average distance between plug points is equal to 2.75 ft. in shale and 1.5 ft. in sandstone. Two core samples, a vertical and a horizontal, were taken in every plug point. Plugs' diameter is 0.75 in., the length is equal 0.5 or 1.25 in.

Preparation of the plugs was conventional for AMOCO PRC Rock's Properties Laboratory. A program of the measurements and their current status are shown in Table 2.

Table 2

Status of Rock's Properties Measurements As Of June 27, 1994

Measurement Of	Status	Number of Samples
Grain Density	Done	106 of Sandstone
Permeability	Done	103 of Sandstone
FTIR Spectroscopy	In Progress	-
Sonic and Ultra Sonic Velocities	In Progress	-

Summary statistics of the available data are represented in Table 3.

Table 3

Summary Statistics Of Rock's Properties

Property	Units	Number of Plugs	Minimum Value	Maximum Value	Average Value	Median	Standard Deviation
Grain Density	g/cm.c	106	2.267	2.731	2.645	2.655	0.0555
Porosity	%	103	7.6	23.8	16.16	16.90	4.22
Vertical Permeability	mD	52	0.001	331	56.8	15.24	89.9
Horizontal Permeability	Md	52	0.018	413	84.5	29.1	112.4

The main results of statistical analysis are the following:

1. There is no correlation dependence between grain density and the other available rock's properties or between grain density and the depth.
2. Permeability and porosity of sandstone are increased with the depth. This fact may be explained by alteration of grain size with the depth due to change of depositional conditions.
3. Horizontal permeability is approximately 30-40% higher than vertical permeability. See Table 3.
4. There is a strong correlation between permeability and porosity.

Engineering Description and Flow Simulation
(By Asnul Bahar, Leslie Thompson and Mohan Kelkar)

Geological Simulation

Based on the new DGI description of the geological interpretation, a new geostatistical simulation was conducted to replicate this description. A program called GTSIM[1] has been used instead of SISIMPDF[2] as used previously. The GTSIM is the Gaussian Truncated Simulations of Lithofacies. The complete methodology of GTSIM can be found in the SCRF May-1993 Report[1]. There are two main advantages of using this program that are applicable to this problem, they are :

- •The ability to incorporate the proportionality of each DGI at a certain vertical depth.
- •The computation time.

The proportionality of each DGI means the probability of a DGI to exist at a certain depth. This proportionality curves control how much each DGI should present at a depth. Figure 8 shows the input of proportion curve, as provided by the geologist, for the Self Unit. The program GTSIM honors this proportion curve as well as the spatial relationship. Figure 9 shows the proportion curve of the simulation output. It can be observed that they match very well.

Before a complete GTSIM run can be made, the spatial relationship of each DGI, in the form of variogram, has to be determined. The conditioning data to generate the variograms were taken from the available logs. The log data did not reveal any areal anisotropy. However, the sand maps provided by the geologist clearly showed a certain direction of channel flow, such as channel in DGI-A, C, and D. Using these two facts, it was decided to run the simulation in two cases, i.e. Case-1 where the areal DGI distribution was assumed isotropic (in horizontal plane) and Case-2 where DGI-A, C, and D were assumed to be anisotropic in horizontal plane. For Case-2, the major direction of continuity for DGI-A was assumed 110 degree, for DGI-C it was 45 degree, and for DGI-D it was 30 degree. These directions were based on geologists interpretation of individual units.

As a cross validation, the results from the simulation for Case-2 were compared with the core data of well #28, 31, 32, 37, 43, 47, and 82. The data from these wells were never used in the conditioning data. The results for well #43, and #82 are presented in Figure 10. It can be observed that the match is reasonable.

Porosity Description

The porosity description was generated using simulated annealing method. The details about simulated annealing method can be found elsewhere.[3] To get a general porosity description, the program has been run for each of the DGIs by assuming that the reservoir contained by that DGI only. Then a filtering process was implemented to generate the real porosity description for the reservoir. The filtering is a process where the type of the DGI was checked for every grid block and then the porosity corresponding to that DGI was assigned to that grid block. A value of zero was assigned to grid block of shale. The generated porosity was compared with log porosity at well #82. The match is excellent.

Permeability Description

As mentioned in the last report, one of the difficulties we encountered in our reservoir description process is the limited permeability data. It was observed that the linear relationship between porosity and log permeability did not exist. To generate permeability distribution, we used a method of conditional distribution.

In this procedure the permeability was assigned to a grid block conditioned both to the type of the DGI and to the porosity value of that grid block. The first step of this procedure is to plot the relation between the porosity and permeability for each of the DGI (A through F). The second step is to divide each of this relationship into several porosity classes. For each of these porosity classes, the cumulative conditional distribution for permeability is calculated. The last step is to assign a permeability value to a grid block. This is done by first selecting a suitable CDF Plot which corresponds to the type of the DGI and the value of the porosity. Knowing the CDF for that grid block a random permeability value within that class is assigned.

Figure 11 presents the comparison between the simulation and the core permeability data of well #82. The comparison is very good. To further validate this permeability description, the results were compared with the well test interpretation. The results of the well test are shown below.

Table 4 Well Test Results				
No.	Well #	*kh* (mD.ft)	Completion Zone	Remarks
1	54	170	A, B, C	Boundary Effect
2	60	133	A, C, D, E	Boundary Effect
3	61	1531	C, D, E	No Boundary Effect
4	63	495	A, B, C, D	Boundary Effect
5	64	190	B, C	Boundary Effect
6	69	176	B, C	No Boundary Effect

In order to compare the Permeability-Thickness Product (kh) of the well test and the simulation, the following procedure was applied :

1. A radius of investigation is defined as half the distance between adjoining wells.
2. The permeability inside this radius was averaged geometrically. The geometric average was calculated only for layers which are perforated.
3. The kh of the simulation then calculated as the summation at each of the layers.

Figure 12 shows this comparison. Except for well #61, where an anomolous result was observed during the well test, the comparison shows a good agreement.

Flow Simulation

In evaluating the performance of the reservoir, the new fluid flow simulation has been conducted. The commercial package ECLIPSE was used as before. Besides the new reservoir description, there are several other revisions applied to the simulation. This is due to the new finding of data/information, such as :

1. Perforation Interval at some wells.
2. Work Over/Reperforation zone(s) at several wells in May-June 1984.
3. Well #50 which has never been completed in Glenn Sand.
4. Fluid Properties as measured at NIPER - Lab. - Bartlesville, Oklahoma.

Due to hardware limitation, the upscaling of reservoir description has to be done before the flow simulation can be run. The geostatistical simulation was conducted using 256000 grid blocks (40x40x160), but the flow simulation can handle 6400 grid blocks only. The reservoir configuration was then reduced to 20x20x16. By observing the average thickness of each DGI then it was decided to use variable grid size in z direction. The grid-block size from top to bottom is 15, 15, 10, 5, 5, 5, 5, 5, 5, 5, 5, 10, 10, 20, 20, 20 ft. the arithmetic average was used for porosity either for horizontal or vertical blocks, while the following procedure was applied for permeability.

1. Permeability average in either X or Y direction (Kx or Ky).

   •The permeability generated by geostatistics simulation was assumed to be the permeability in the horizontal direction ($Kx = Ky = K$simulation).

   •For blocks in the horizontal plane :

   -Two harmonic averages (kh_1 and kh_2) were calculated for 2 pair blocks in the direction of flow, as follows :

$$kh_i = \frac{2kx_1 kx_2}{kx_1 + kx_2}$$

   -The super block average is calculated as the arithmetic average of kh_1 and kh_2, as follows :

$$k_x = k_y = \frac{kh_1 + kh_2}{2}$$

   •The arithmetic average then was used to calculate the average for vertical blocks.

2. Permeability Average in Z direction (Kz)

   • Kz is assumed to be 1% of Kx.

   •Harmonic average kh_i was calculated for blocks in the direction of flow (vertical direction).

   •The super block average for Kz is calculated as the arithmetic average of the 4-neighbor horizontal blocks.

In the previous report, it was assumed that the initial production occurred with Bottom Hole Pressure (BHP) of 400 psi, and was assumed uniform throughout the field. A new run of simulation has been made with variable BHP to get a better match of the initial potential. It can be seen that the match is very good. Following the fact that the non-uniform BHP is a better approach then the simulation was run until 1945 where the gas repressuring treatment was started. The comparison between the simulation results and the observed field performance is shown in Figure 13. The match is reasonable.

We will continue to investigate the simulation results more carefully. The bottom hole pressure as measured in the well test and the oil saturation of well #82 will be compared with the Simulation result. Then, based on the oil saturation map, different strategies will be studied to see the possibility of enhancing the oil recovery of the Self Unit. Such study is still in progress.

References

1. Xu, Wenlong, and Journel A. G., GTSIM: "Gaussian Truncated Simulations of Lithofacies," Report-6 Stanford Center For Reservoir Forecasting, May-1993.

2. Deutsch, C. V. , and Journel A. G.: GSLIB, Oxford University Press, New York, 1992.

3. Perez, G.: "Stochastic Conditional Simulation for Description of Reservoir Properties," Ph.D. Dissertation, The University of Tulsa, Tulsa-OK, 1991.

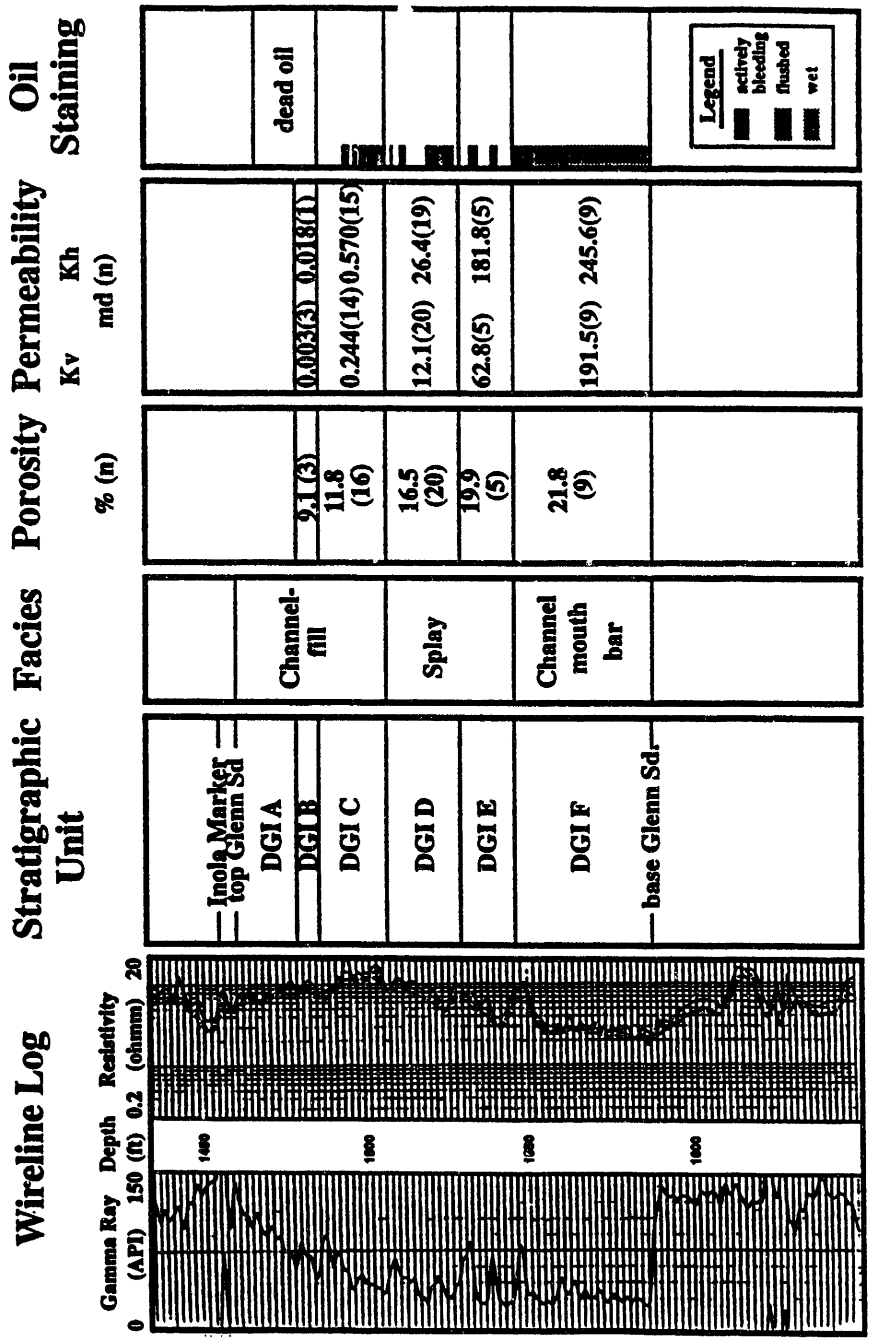

Figure 1: Uplands Self No. 82 well summary. Stratigraphic units include the stratigraphic marker bed (Inola) and the discrete genetic intervals (DGI) that make up the Glenn Sand. Permeability values are geometric means for each DGI sampled (n=number of samples) with reference to air through conventional core plugs.

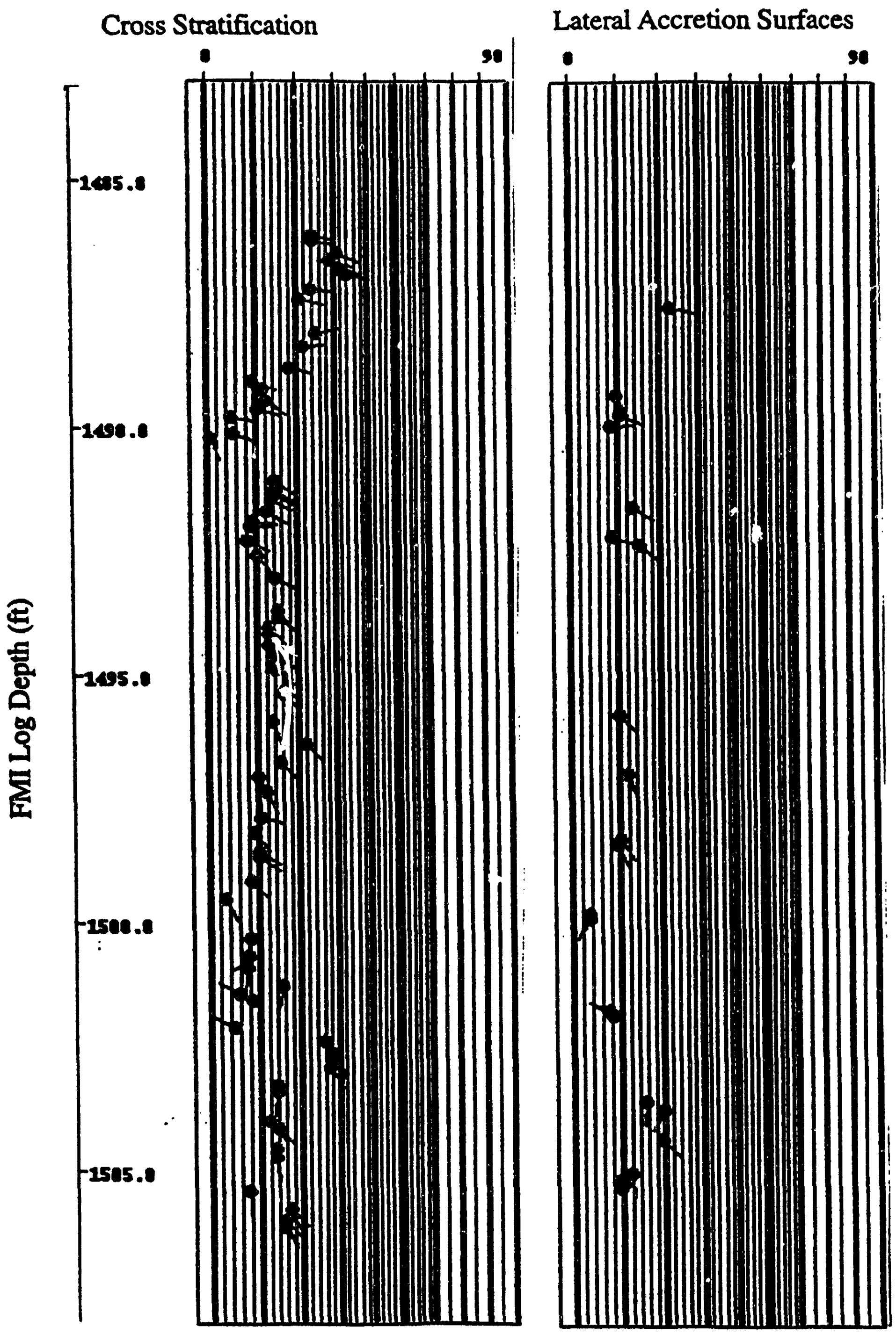

Figure 2: Uplands Self No. 82 well tadpole plots from FMI analysis for DGI C. The tadpole "body" is located at the scaled dip angle (in degrees from horizontal), and the tadpole "tail" is pointing in the dip compass direction.

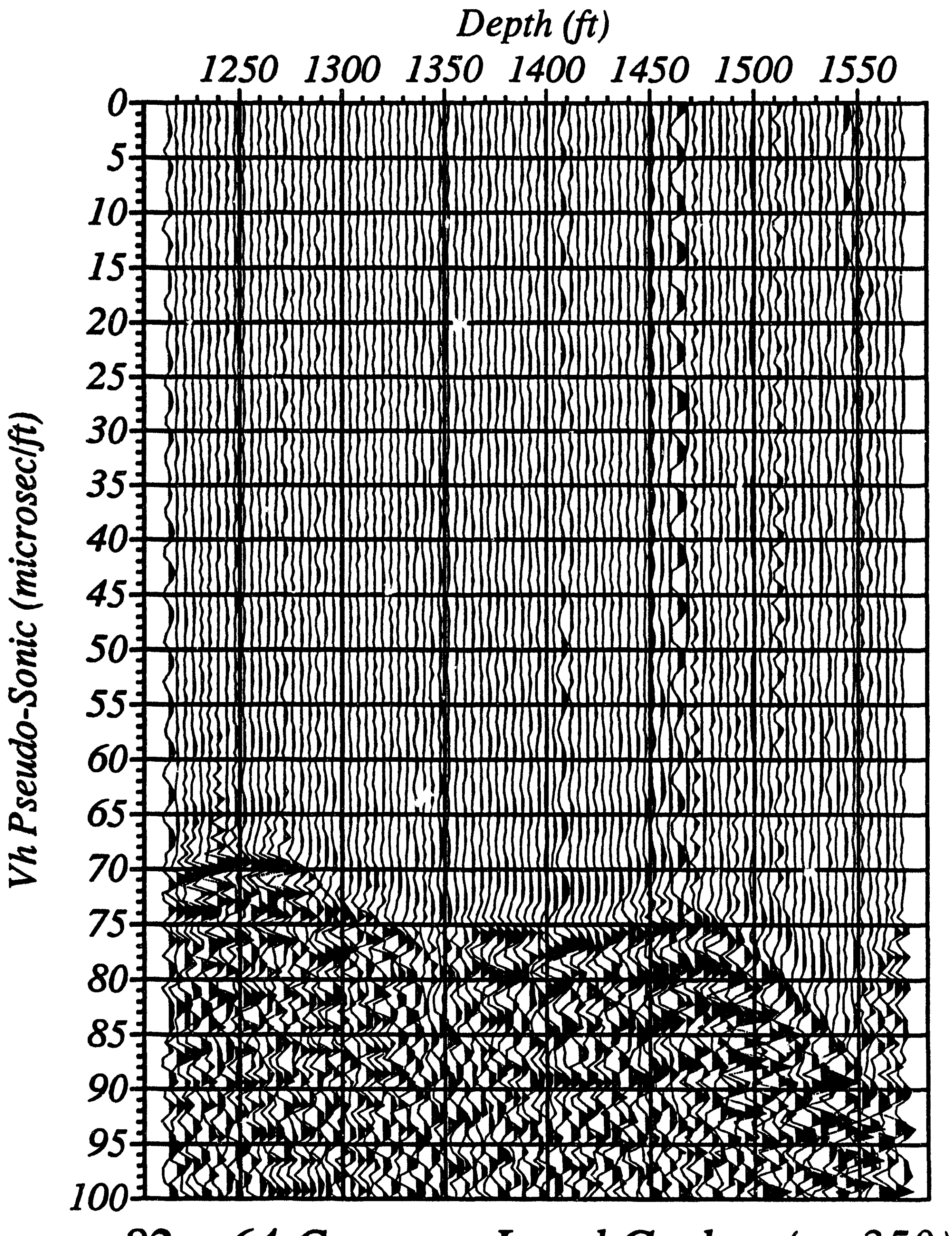
Depth (ft)
1250 1300 1350 1400 1450 1500 1550
0
5
10
15
20
25
30
35
40
45
50
55
60
65
70
75
80
85
90
95
100
Vh Pseudo-Sonic (microsec/ft)
82->64 Constant Level Gather (x=350)

Figure 3

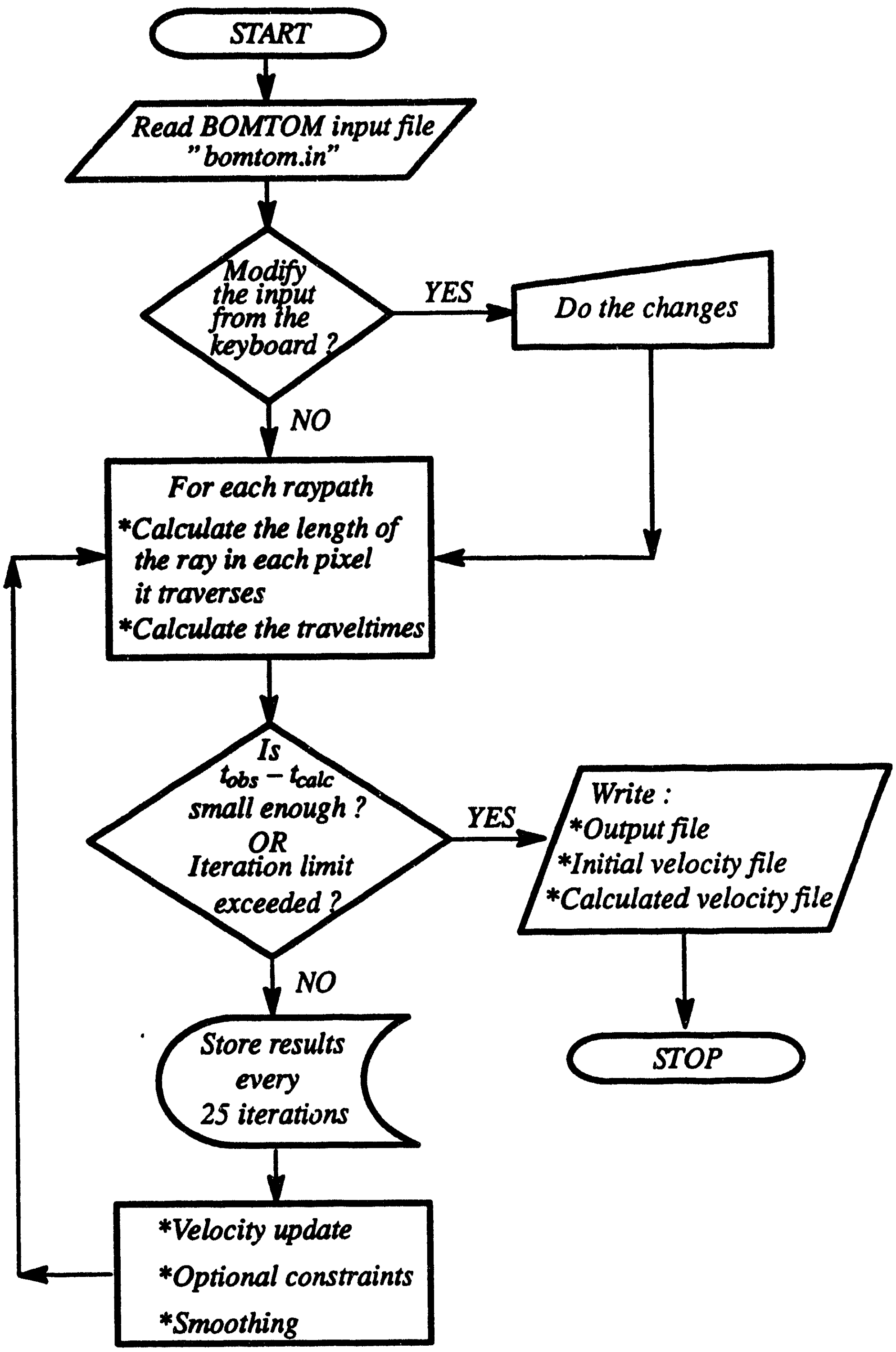

Figure 4: A generalized flowchart of BOMTOM.

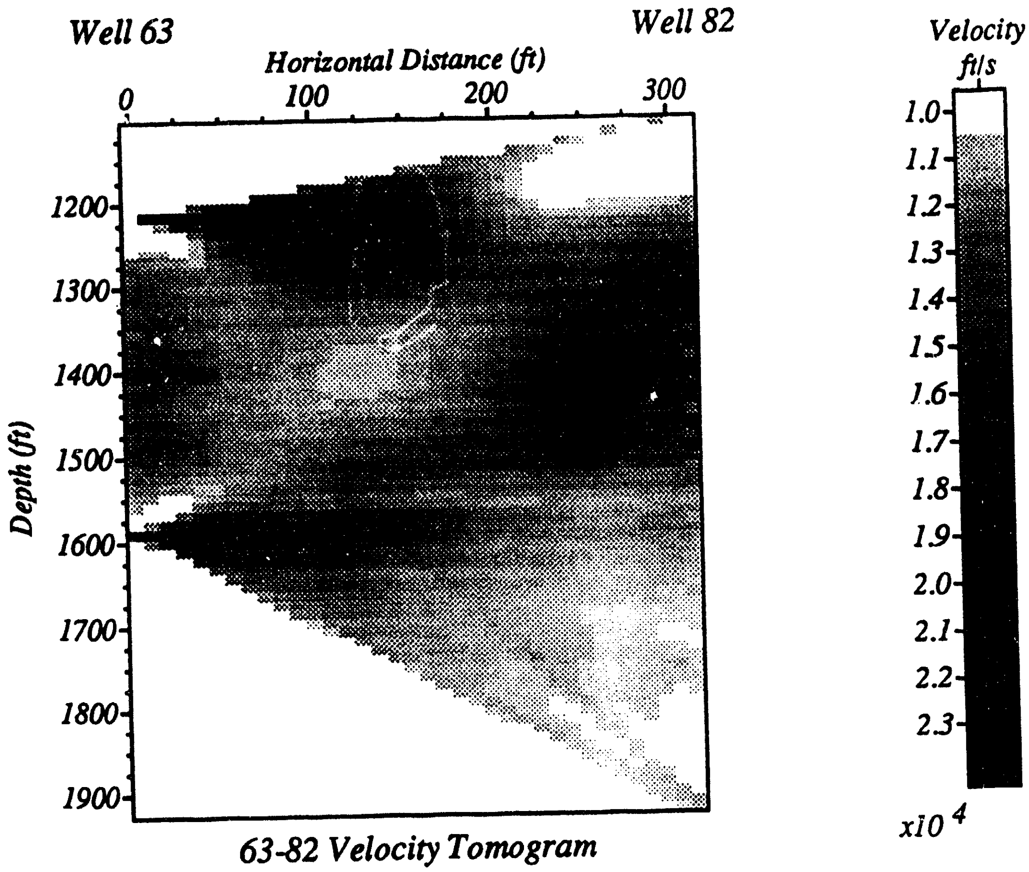

Figure 5: TU velocity tomograph between wells #63 and #82.

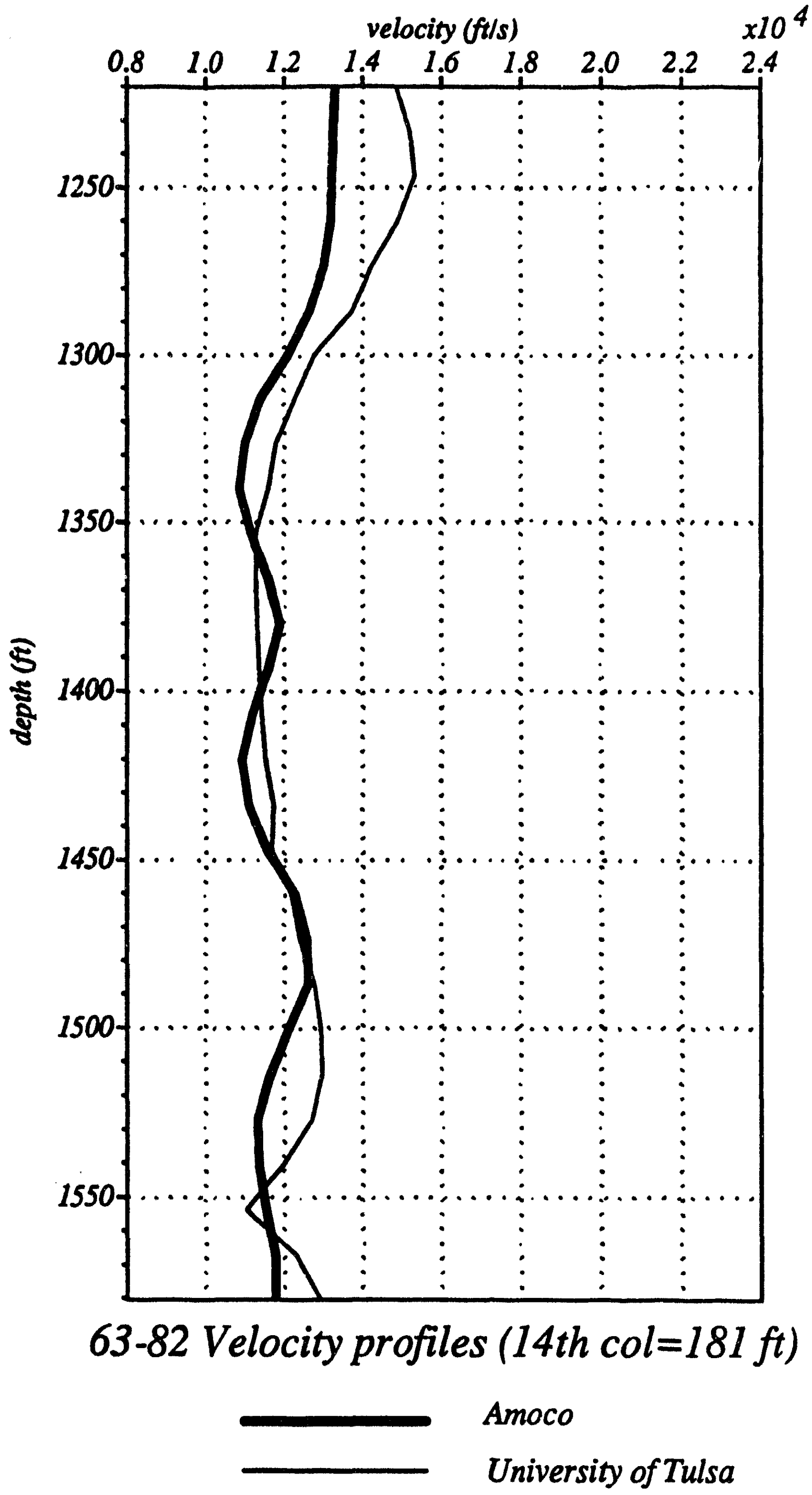

Figure 6: Velocity profile comparison at a distance 181 ft. from well #63.

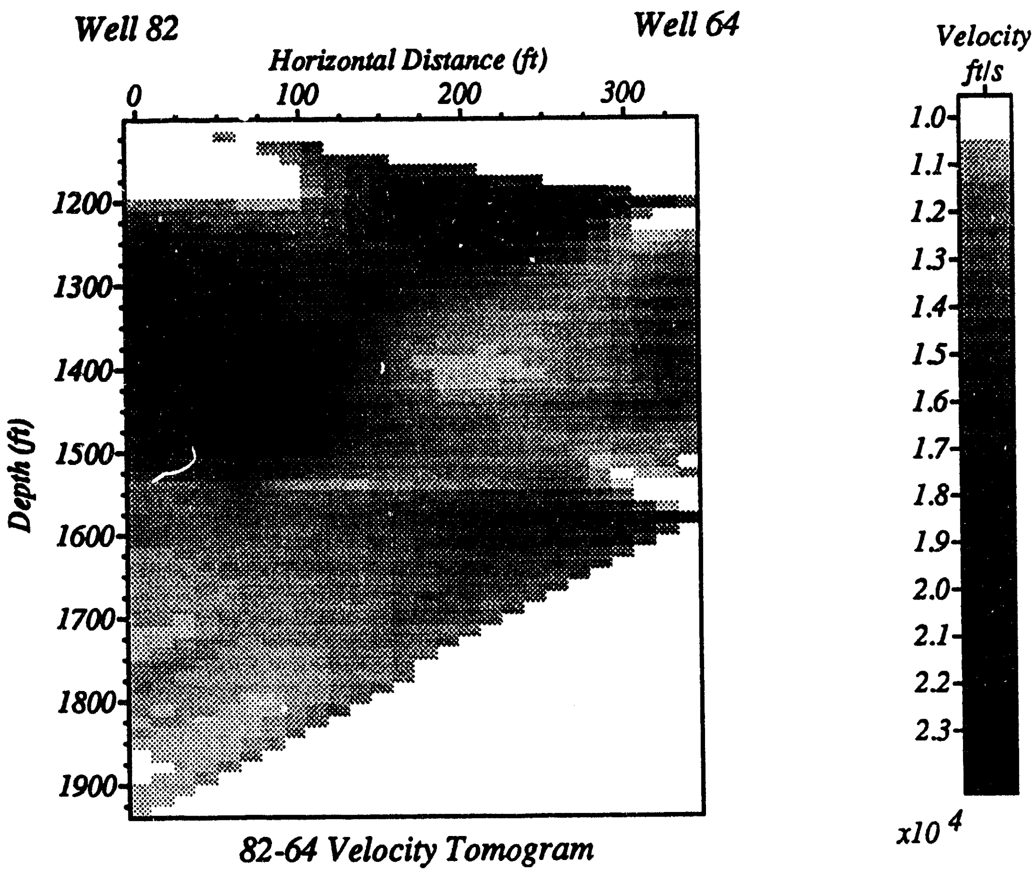

Figure 7: TU velocity tomogram between wells #82 and #64.

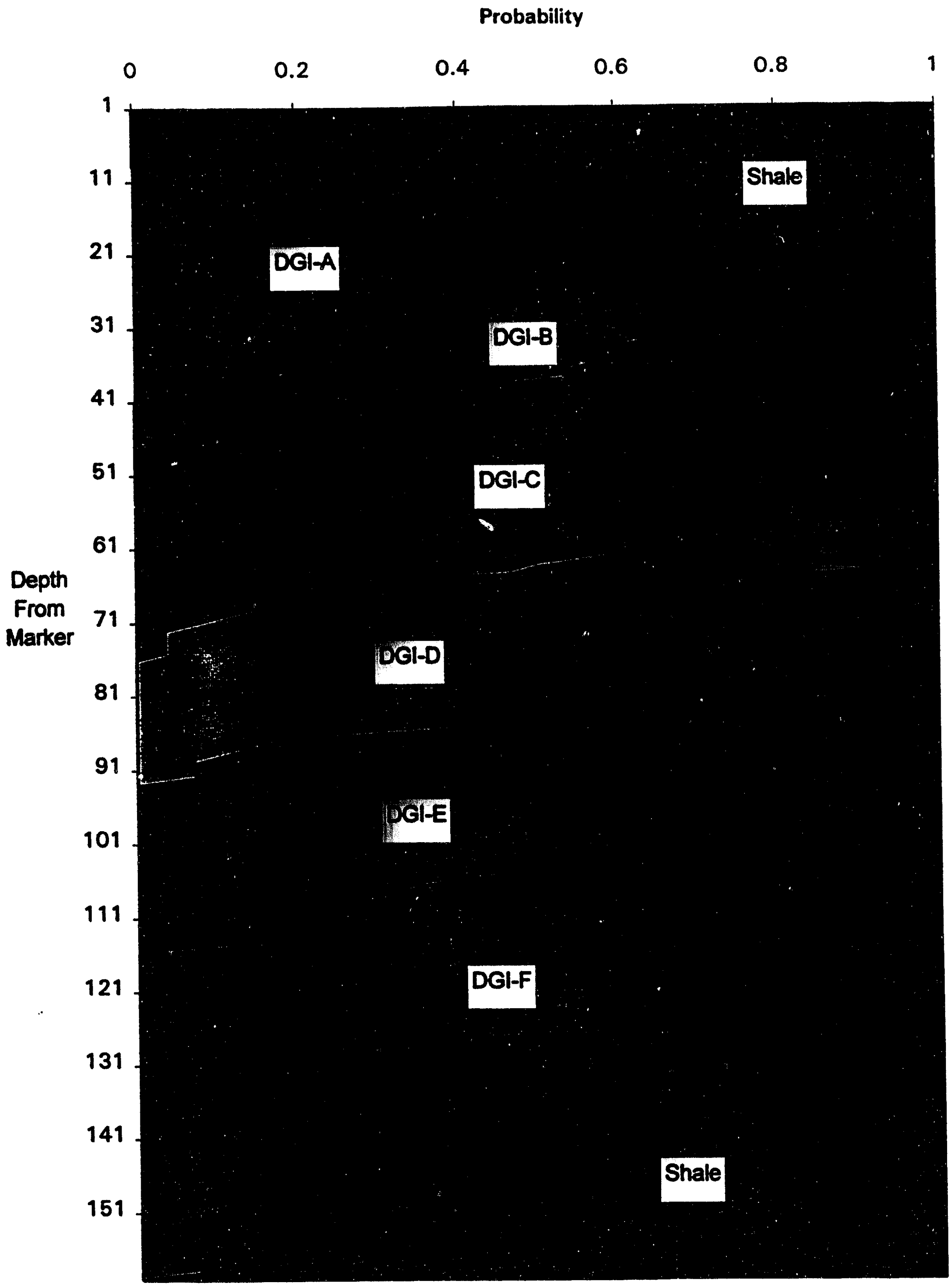

Figure 8: Input proportion curve as provided by the geologist.

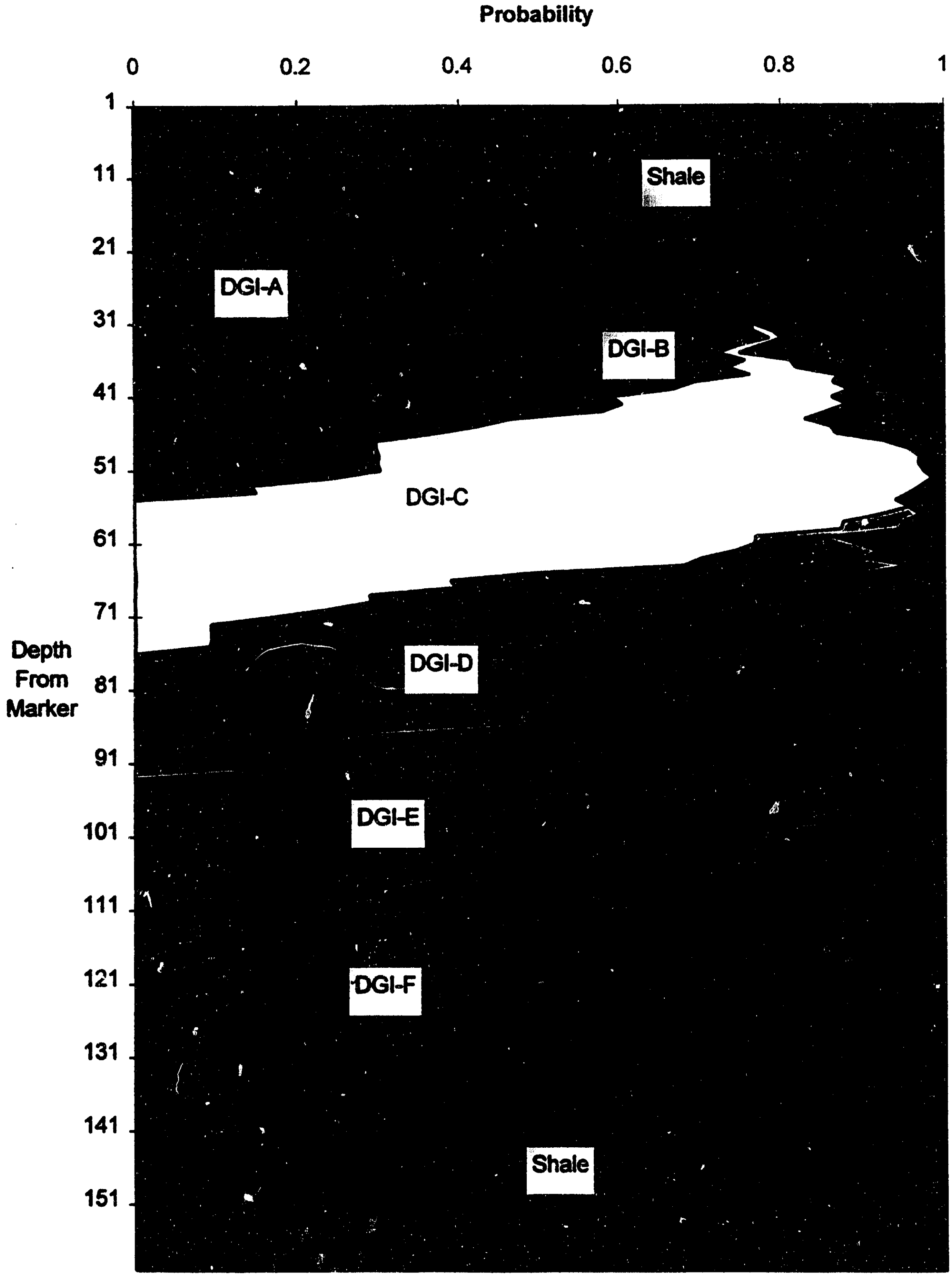

Figure 9: Output proportion curve from the simulation.

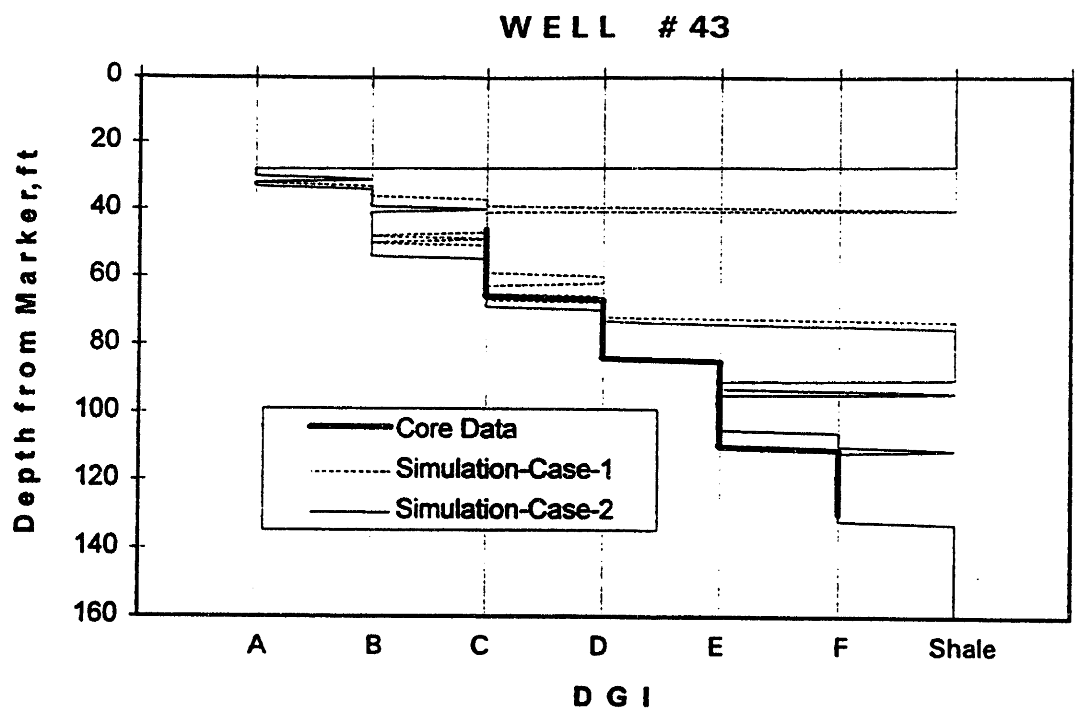

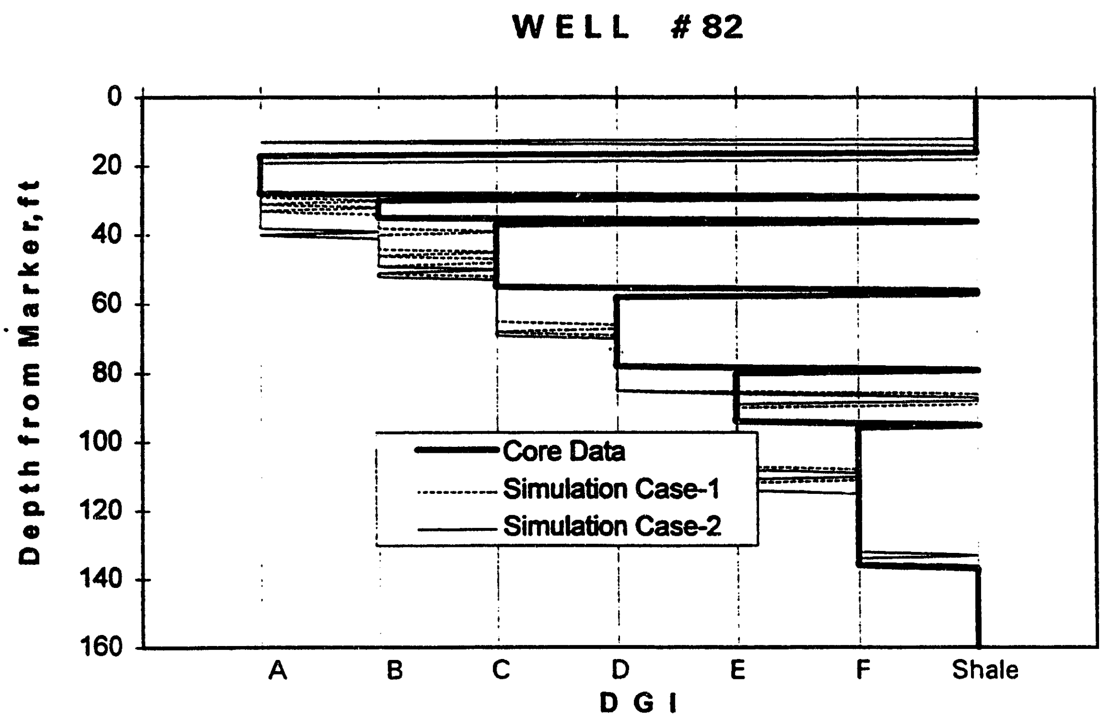

Figure 10: DGI comparison between core data and the simulation for well #43 and #82.

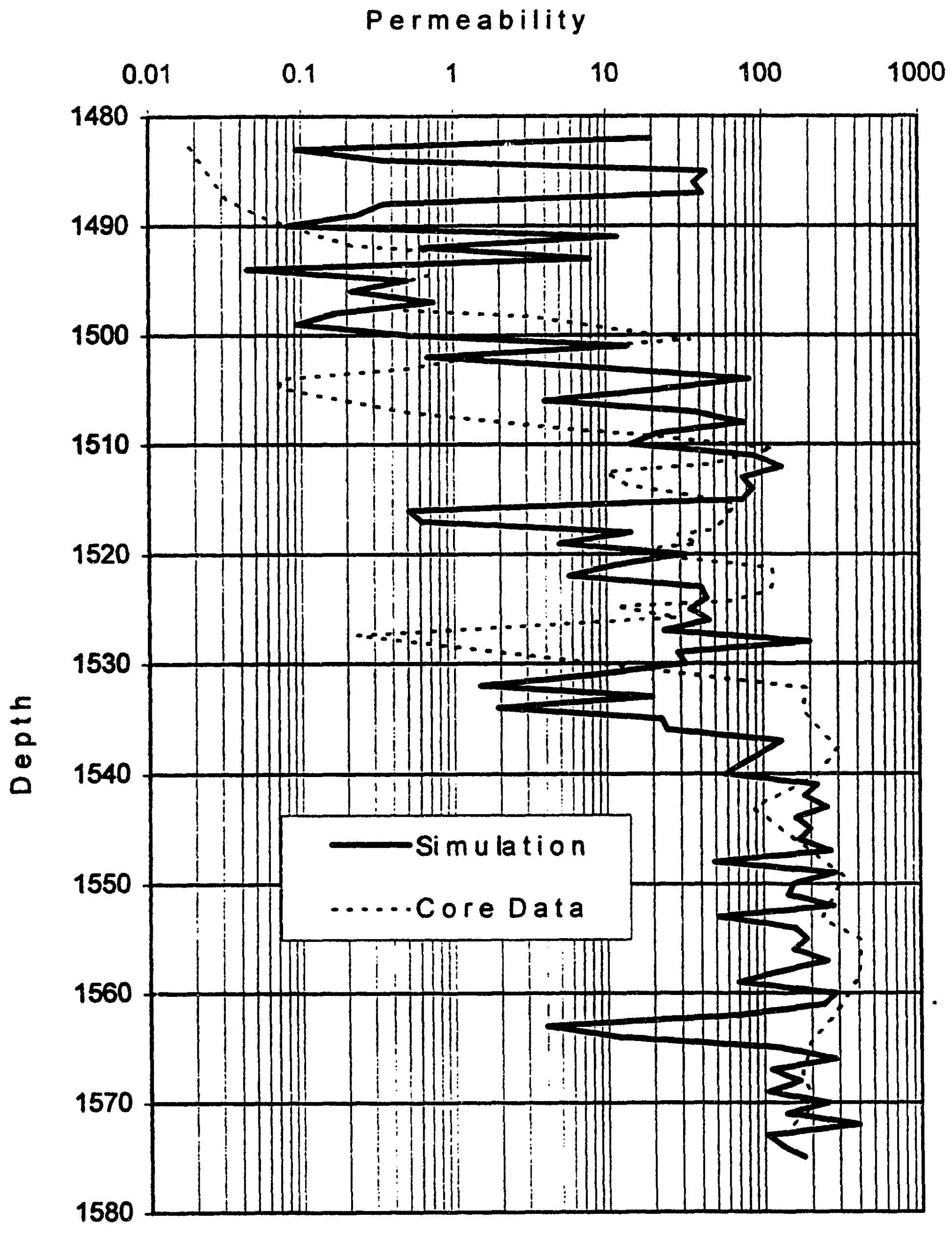

Figure 11: Comparison of the permeability at well #82 between the core data and the simulation.

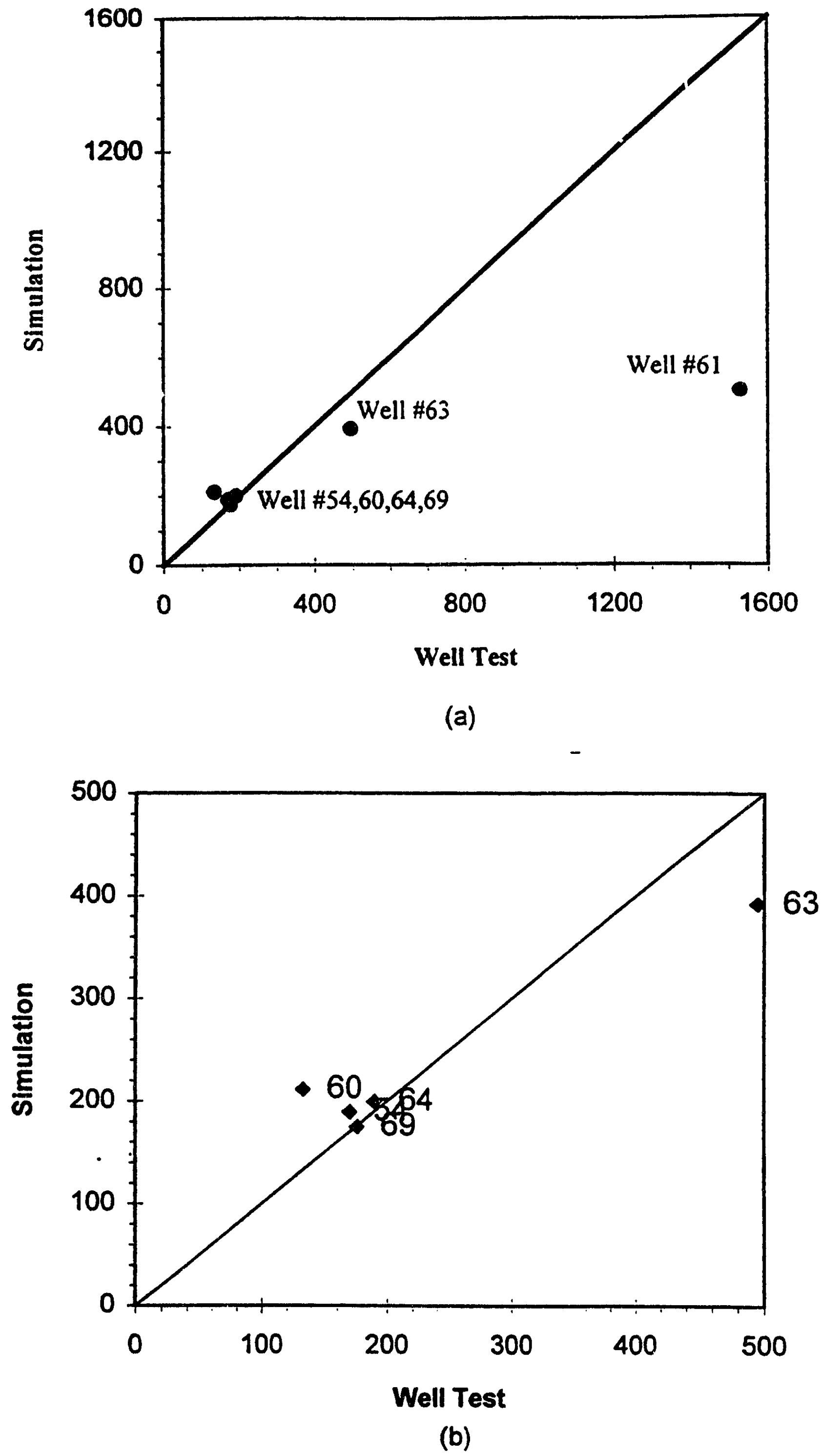

Figure 12: Comparison of the permeability-thickness product (kh) between well test and simulation. Figure 12(a) presents all tests wells where Figure 12(b) excludes well #61.

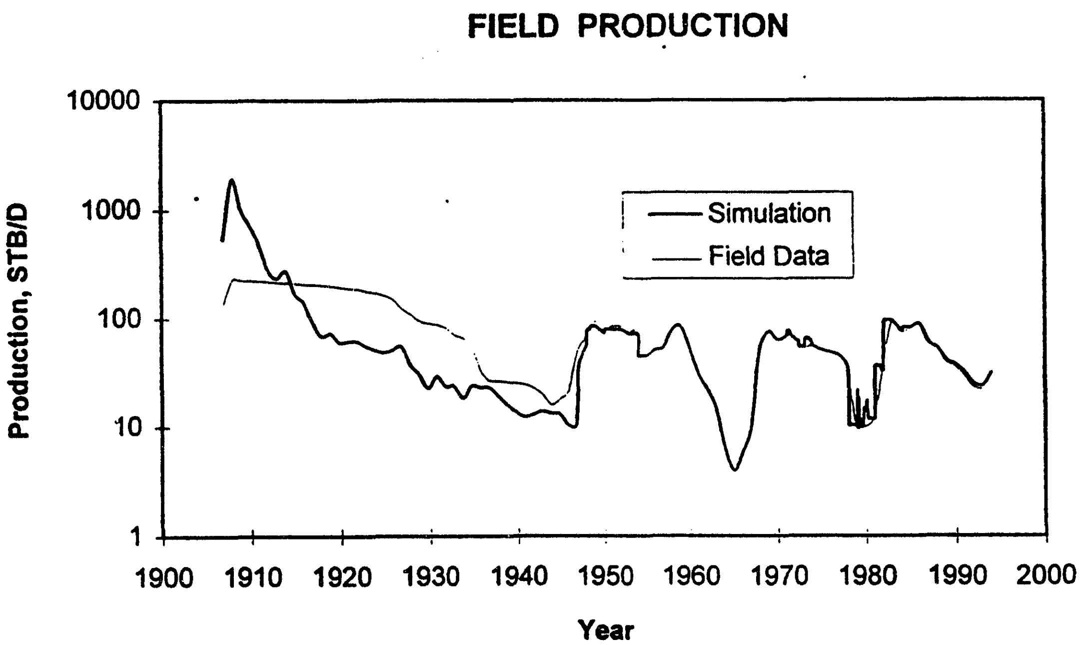

Figure 13: Oil production comparison between field data and simulation.

DATE
FILMED
10/17/94

END